ACS APPLIED MATERIALS & INTERFACES

Organic Electronic Devices

Lightweight and Bulk Organic Thermoelectric Generators Employing Novel P-type Few Layered Graphene Nano-flakes

Saqib Rafique, Matthew Richard Burton, Nafiseh Badiei, Jorge Eduardo Gonzalez-Feijoo, Shahin Mehraban, Matthew Carnie, Afshin Tarat, and Lijie Li

ACS Appl. Mater. Interfaces, **Just Accepted Manuscript** • DOI: 10.1021/acsami.0c06050 • Publication Date (Web): 11 Jun 2020

Lightweight and Bulk Organic Thermoelectric Generators Employing Novel P-type Few Layered Graphene Nano-flakes

Saqib Rafique[1], Matthew R. Burton[2], Nafiseh Badiei[1], Jorge Gonzalez-Feijoo[1], Shahin Mehraban[3], Matthew J. Carnie[2], Afshin Tarat[4*], and Lijie Li[1*]

[1]*Multidisciplinary Nanotechnology Centre, College of Engineering, Swansea University, Swansea SA1 8EN, United Kingdom*

[2]*SPECIFIC, College of Engineering, Swansea University, Swansea SA1 8EN, United Kingdom*

[3]*Materials Advanced Characterization Centre, Future Manufacturing Research Institute, College of Engineering Fabian Way, Crymlyn Burrows, Skewen, Swansea SA1 8EN*

[4]*Perpetuus Carbon Technologies Ltd., Unit B1, Olympus Ct, Mill Stream Way, Llansamlet, Swansea SA7 0AQ, United Kingdom*

*Corresponding authors: l.li@swansea.ac.uk , afshintarat@perpetuuscarbon.com

ABSTRACT

Graphene exhibits both high electrical conductivity and large elastic modulus, which makes it an ideal material candidate for many electronic devices. At present not much work has been conducted on using graphene to construct thermoelectric devices, particularly due to its high thermal conductivity and lack of bulk fabrication. Films of graphene-based materials, however, and their nanocomposites have been shown to be promising candidates for thermoelectric energy generation. Exploring methods to enhance the thermoelectric performance of graphene and produce bulk samples can significantly widen its application in thermoelectrics. Realization of bulk organic materials in the thermoelectric community is highly desired to develop cheap, Earth-Abundant, light, and non-toxic thermoelectric generators. In this context, this work reports a new approach using pressed pellets bars of few layered graphene (FLG) nanoflakes employed in thermoelectric generators (TEGs). Firstly, FLG nano-flakes were produced by a novel dry physical grinding technique followed by graphene nano-flakes liberation using plasma treatment. The resultant material is highly pure with very low defects, possessing 3 to 5-layers stack as proved by Raman spectroscopy, X-ray diffraction measurement and scanning electron microscopy. The thermal and electronic properties confirm the anisotropy of the material and hence the varied performance characteristics parallel to and perpendicular to the pressing direction of the pellets. The full thermoelectric properties were characterized both parallel and perpendicular to the pressing direction, and the proof of concept thermoelectric generators were fabricated with variable amounts of legs.

KEYWORDS: Few layered graphene, bulk thermoelectric generator, high output power, flexible substrate, organic

1. INTRODUCTION

Global energy consumption has dramatically increased over the past few decades and if the world pursues along its present path then the consumption is predicted to grow 20–30% by 2040 and beyond, largely dominated by the fossil fuels.[1] Owing to the fast depletion of the current affordable energy resources, sustainability is critical as the world energy demand is increasing. Moreover, the energy produced from conventional fossil fuels is accompanied by environmental constraints such as the greenhouse effect and the air pollution.[2] Almost two-thirds of the total energy produced is dissipated in the environment as heat,[3-4] which highlights the potential of thermoelectric (TE) generators. TE devices allow for the direct conversion of heat to electricity through a temperature gradient. The heat can be harvested from multitude sources such as waste heat from factories, engines, electronic devices and even the human body. [5-6]

The efficiency of a TE material is evaluated by the dimensionless figure of merit, $ZT = S^2\sigma T/\kappa$, where S, σ, T and κ denote the Seebeck coefficient (V K^{-1}), electrical conductivity (S m^{-1}), absolute temperature (K) and thermal conductivity (W m^{-1} K^{-1}), respectively.[7-8] The transport characteristics are interrelated, thus optimizing one variable conflicts with another.[9] This leads to optimal TE materials typically being heavily doped inorganic semiconductors such as Bi_2Te_3, PbTe and SiGe, which exhibit some of the highest *ZT*s, typically above 1.[10-13] To date there has been limited uptake in thermoelectrics due to the components have serious drawbacks of toxicity, material scarcity and relatively higher cost, which ultimately has limited their widespread commercialisation.[14] Conversely, conducting polymer-based organic TE materials have gained significant interest due to their unique advantages of abundance, low cost of constituent elements, facile processing, mechanical flexibility, intrinsically low thermal conductivity and relatively lower toxicity.[15-19] However, their performance is significantly lower than the conventional

inorganic TE materials, as the power factor of organic materials is limited by the low *S* and often low σ.[20] Due to the low Seebeck coefficient values of conducting organic polymers, the resulting *ZT*s of these materials are substantially lower than bulk inorganic materials, with a *ZT* of 0.42 published several years ago not being surpassed.[21] Moreover, it is hard to extract bulk-materials required for traditional thermoelectric generators (in the order of 1 mm × 1 mm × 2 mm) from these organic polymers, due to cost of synthesising the polymers and it being only possible to obtain only a few hundred nanometres thickness of the deposited films using any of the deposition techniques which are required for high σ values. These limitations highlight the need for new Earth-abundant and low-cost organic solutions.

Graphene, a single layer of a carbon in a two-dimensional hexagonal lattice,[22] being the most widely explored instance of 2D materials, has gained remarkable attention for its applications in mechanical, electrical and photonic industries owing to its unique properties.[23] For instance, It possesses very high carrier mobility (~200000 $cm^2/[V.s]$), excellent mechanical strength and electrical properties.[24] Graphene possesses better electrical conductivity and larger surface area compared to other nanocarbons.[20] Graphene, however, as a TE material has limited scope owing to the semi-metallic nature of graphene that implies limited *S*,[25] along with the high κ that lead to the modest TE conversion efficiency.[26] A number of theoretical studies suggested various nanostructured designs to circumvent these problems such as graphene nanoribbons,[27] heterostructures [28] and nanopore structures [29] to yield high *S* values. Although, a few of these approaches showed promising output and unusually predicted larger *ZT* values for graphene,[25] most of them remained a challenge to develop a practical device owing to the deficiency of desired large-area fabrication techniques.[30] As a result, despite the exceptional promise of graphene as the constituent in the polymer-based low-temperature thermoelectrics,[30-31] only a few studies have

focused on all graphene-based thermoelectrics.[32] Particularly, its potential for bulk material synthesis coupled with its mechanical resilience, highlight its potential for bulk thermoelectrics. An area that to date has been unexplored.

In the context of the above discussion, the present work demonstrates novel few layered graphene (FLG) nano-flakes based pellets, with the capability to manufacture pellets of up to 10 cm × 10 cm × 10 cm. These can then be used in bulk TE device applications. The utilized FLG was sourced from a novel dry physical grinding technique followed by graphene nano-flakes liberation using plasma treatment, intercalation with Dielectric Barrier Discharge (DBD) utilizing both atmospheric and Vacuum process. The resulting pellets exhibit anisotropic properties parallel to and perpendicular to the pressing directions, with electrical conductivity similar to the best conducting organic polymers being observed. The lightweight bulk thermoelectric materials could be of significant interest to thermoelectric applications where weight is a concern, such as transport. Moreover, the synergy of the lightweight bulk pellet material and the flexible substrate used in this work, highlights its potential for use in wearable systems.[33]

2. EXPERIMENTAL SECTION

2.1 Materials Synthesis

FLG nano-flakes (Figure 1a) were produced by a novel dry physical grinding technique followed by graphene nano-flakes liberation using plasma treatment, intercalation with Dielectric Barrier Discharge (DBD) utilizing both atmospheric and vacuum processes. In graphene-like structures, due to the 90° rotation of a C–C bond, Stone–Wales defects introduction results in a change in six-membered rings into typically pentagons and heptagons. (5-7 carbon). The density of Stone–Wales defects is relatively smaller due to the high activation barrier of multiple electron

volts (eVs) for the bond rotation. The defects in all probability facilitate partially or completely negation of the Van Der Walls forces. Argon plasma was employed to generate defect sites for the functionalization with a variety of moieties allowing plasma induced ion intercalation to further cause the Van Der Waals attraction to become a Van Der Waals repulsion negating the bonds that hold that graphene sheets within the graphite.

2.2 Materials Characterization

Morphology and structural properties of the FLG nano-flakes were characterized using field emission scanning electron microscope, FESEM (Hitachi 4800 S, Japan) equipped with an Oxford Instruments EDS attachment and a Renishaw inVia Qontor confocal Raman spectrometer using a CW He-Ne laser emitting at 633nm with a power of 500 mW, respectively. The Raman shifts were calibrated using an optical phonon frequency (520.6 cm^{-1}) of single silicon crystal. In addition, the reflecting microscope objective was set to be 50×, n. a. 0.15, and the excitation spot diameter was 15 μm. The light was detected by a charge-coupled device. X-ray diffraction (XRD) was carried out using a Bruker D8 diffractometer with Cu-Kα radiation.

2.3 Thermoelectric Characterization

The Seebeck coefficient and the electrical properties of free-standing pressed pellet-bars were measured both parallel to and perpendicular to the pressing direction using an ULVAC ZEM-3 with a helium atmosphere. The Thermal Diffusivity of the sample was measured using a Netzsch LFA 457. The solid Ø12.5mm sample was placed in aluminium titanate sample holder with a silicon carbide cap. The sample was located in the high temperature furnace chamber which was evacuated and back filled with Argon. A sustained flow of 100 mL per minute of Argon cover gas was then piped through the chamber throughout the experiment. The temperature change of the sample was detected using an InSn-IR detector cooled by liquid nitrogen. Temperature steps of 50

°C were taken from 35 °C to 1000 °C. Five shots were performed at each temperature step and the standard deviation was calculated. The thermal diffusivity of each shot was calculated using the Cowon method with pulse correction applied.[34] Heat capacity was determined from Differential scanning calorimetry (DSC) (**Figure 2e**), with the method described in detail in the supporting information. The bulk density was determined to be 2.178 g cm^{-3} using the method of hydrostatic weighing, employing Archimedes' principle.[35]

2.4 Fabrication of Thermoelectric Generators (TEGs)

Firstly, 1 g of FLG nano-flakes were pressed with the SGS 20 Ton Hydraulic Press - Hand Pump at 10 tons per square inches force to obtain FLG sheets measuring 5.0 cm × 5.0 cm × 0.065 cm each. Further, these sheets were sliced into the pressed pellet-bars measuring 3.0 cm × 0.5 cm × 0.065 cm. The thicknesses of the FLG pellet bars was measured to be ~ 0.65 mm with relative deviation of ± 10% using digital Vernier caliper. Onto the polyester sheet with a thickness of ~ 180 μm (obtained from Customark Ltd. United Kingdom), the parallel legs comprising of pressed pellet-bars of FLG nano-flakes were glued using Loctite double-bubble epoxy glue (Loctite, Germany). Silver conductive paint was brush painted to make top and bottom contacts. The paste was ensured to be completely dried before further characterizations have been made.

2.5 Device Characterization

Thermoelectric devices were measured as follows, the current (I) and the voltage (V) were recorded with a Keithley 2401 digital Multimeter. A digital hotplate model Elektrotechnik PR 53T was used to heat the hot side and a custom-made passive cold stage has been designed to use as heat sink to help maintain a temperature gradient (ΔT). ΔT was determined by using two thermocouples attached to the samples, one on the cold side the other on the hot side. All measurements were taken with 5 seconds of reaching each ΔT.

3. RESULTS AND DISCUSSIONS

Figure 1 shows the molecular structures of the FLG nano-flakes used to fabricate the bulk-FLG TEGs, along with the pellet making process and a photograph of an example of the pellets made. Detailed fabrication and characterization procedures have been described in the Experimental Section.

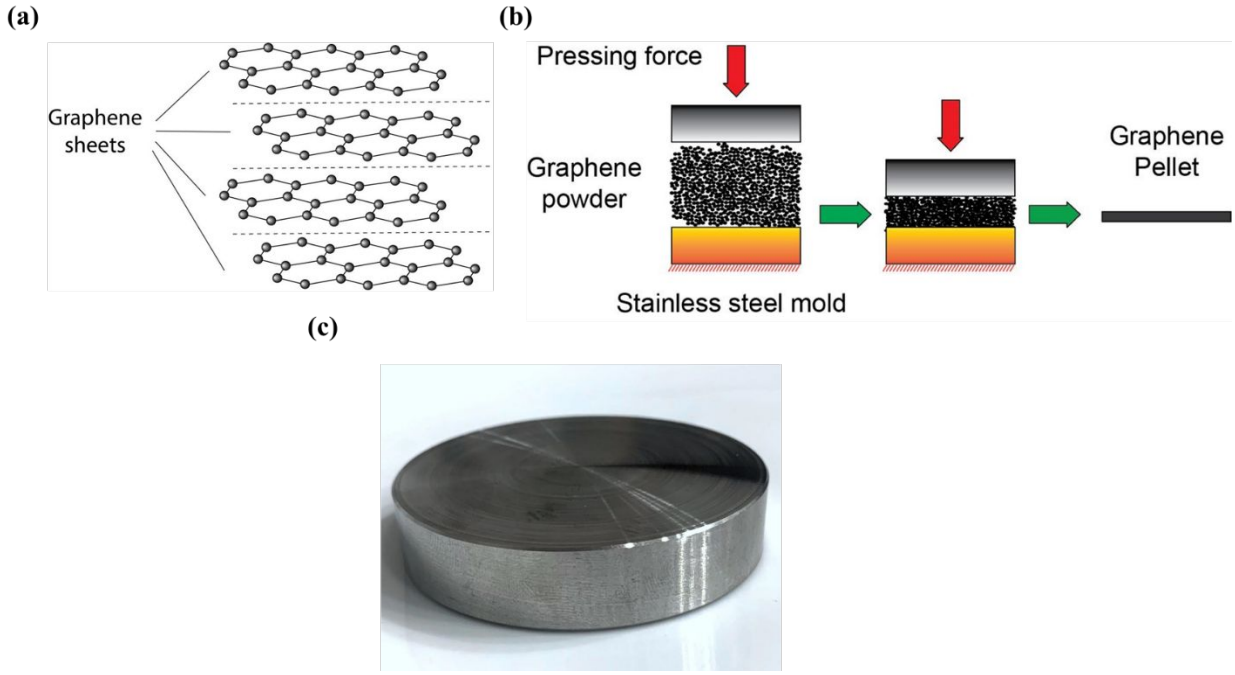

Figure 1: **(a)** Molecular structures of the FLG nano-flakes, **(b)** schematic of the pellet making process from FLG powder, **(c)** photograph of a pellet

3.1 Characterization of FLG nano-flakes

Raman spectral analysis was performed to characterize the prepared FLG nano-flakes, since it is a non-destructive technique to demonstrate the defects and the number of layers through the D, G and 2D bands.[36-37] **Figure 2a** shows the representative Raman spectra possessing the main

peak at 1583 cm^{-1}, which is ascribed to the G band and it represents the doubly degenerate phonon mode of sp^2 carbon[36-37] and this band also validates the existence of graphene as well as to probe the thickness.[38] A very weak Raman scattering peak at 1347 cm^{-1} is ascribed to D-band, which is representative of structural defects in the graphene such as; point defects, dislocation-like defects, bilayer or multilayer bending, substitutional impurities, and carbon adatoms, *etc*., and these defects are attributed to the imperfections in the individual hexagons in the honeycomb structure of graphene.[38] While, the pronounced 2D peak which appears at 2683 cm^{-1} is attributed to the second order of zone boundary phonon.[37] It is noteworthy that greater number of defects in the honeycomb structure induce high peak intensity of D band peak. Also, the intensity ratio of D and G bands, I_D/I_G, increases with the increasing numbers of layers in graphene.[39] However, the prepared material possesses almost no defects as evident from the very low peak intensity of the D-band. Also, the spectra exhibit $I_D/I_G = 0.12$ which is significantly smaller than the previously reported data for FLG such as Lin *et al*.[40] and Rao *et al*.[36] where I_D/I_G ratios to be 0.35 and 0.67 were reported, respectively. All these facts demonstrate the high quality of the prepared material exhibiting very low defects and fewer number of layers. This shows that our FLG is of high quality and exhibits enhanced properties such as excellent electrical conductivity and can be used in wide range of applications including thermoelectrics, solar cells and supercapacitors *etc*.[41-43] This is evident from the diffraction peak at 2θ value of 26.5° of the XRD spectra too, which is ascribed to the 002 crystal lattice and well matched with the JCPDS 41-1487, as shown in **Figure 2b**. Contrary to the broader peak at 26.5° typically attributed to the disordered structure of prepared graphene sheets,[44] the sharp peak (2θ = 26.5°) spanning only within 1° indicates a highly organized crystal structure of the FLG nano-flakes prepared during this work which implies the lesser defects and high quality of our material, also it is consistent with the layer spacing of normal graphite.[45] The

sharp peak is probably attributed to the fact that inner layer spacing within the FLG nano-flakes has a structure identical to that of normal graphite.

The few layered structure has been revealed in the FESEM images too. **Figure 2c** and **d** show low and high magnification images of the FLG nano-flakes, respectively. The FESEM images of graphene nano-flakes show large sized sheets of micrometer dimensions. It seems that several large sheets have been broken into smaller sheets, which might have occurred during the exfoliation process. At higher magnification, ultrathin 2-3 graphene sheets stacked with each other can be clearly seen. While, the inter-sheet spacing is also clearly visible, suggesting a high level of exfoliation which also justifies that our prepared graphene is FLG nano-flakes. This is consistent with our Raman and XRD results too.

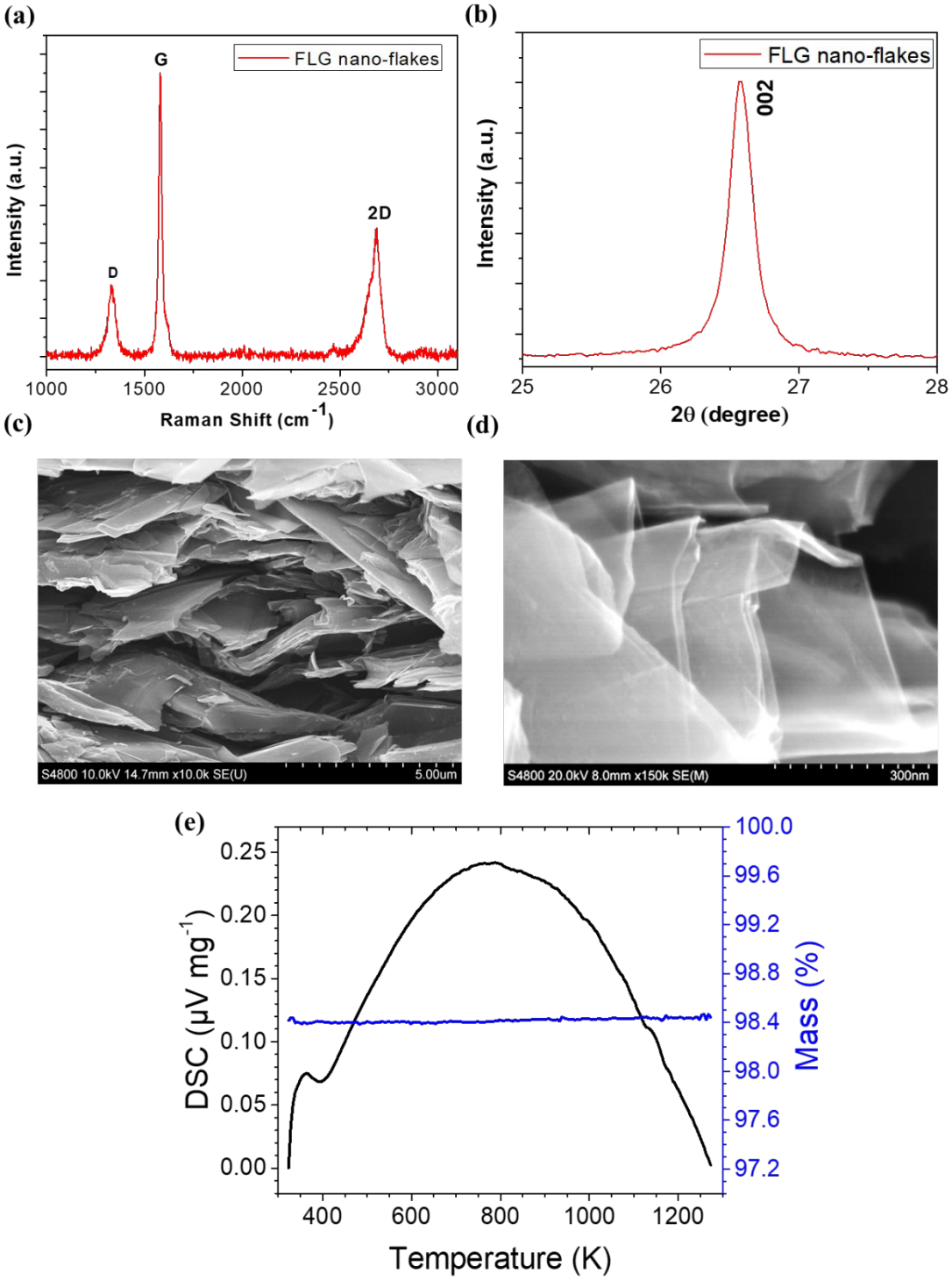

Figure 2: **(a)** Raman and **(b)** XRD spectra along with the **(c)** Low and **(d)** high magnification FESEM images of FLG nano-flakes. **(e)** DSC (black) and thermogravimetric analysis (blue) of bulk FLG.

3.2 Thermoelectric characterization of the FLG nano-flakes based pellets

Thermoelectric characterization of free-standing pressed pellets of FLG can be seen in **Figure 3**. It shows that the electrical conductivity of the material is substantially higher perpendicular to the pressing direction as compared to the parallel to the pressing direction. Both the electrical conductivity and the Seebeck coefficient show a positive correlation with temperature, this observation cannot be explained due to a change in the carrier concentration as these variables are inversely and directly proportional to the carrier concentration, respectively.[46] The plots in **Figure 3a** show perpendicular to the pressing direction an initial value of around 481 S cm^{-1} at 316 K, and an almost linear increase with temperature has been observed leading to a maximum of 1066 S cm^{1} at 1233 K. Whilst, the electrical conductivity showed the similar response parallel to the pressing direction, the values were substantially lower, with a maximum of 176 S cm^{-1} being reached at 1233 K. The non-metallic electrical conductivity dependence on temperature, is most likely a result of scattering of charge carriers at the grain boundaries. This semiconducting behavior type temperature response is consistent with multi-layer graphene in the literature.[47] In contrast, the measurements of the Seebeck coefficients (**Figure 2b**), reveal that the FLG nano-flakes are p-type with metallic-like type behavior. This is evidenced by both the Seebeck coefficient and the electrical conductivity increasing both parallel to and perpendicular to the pressing plane with increases in temperature, with a weak linear trend. This temperature Seebeck dependence observed is believed to be due to a small change in the electrochemical potential and a large degree of hole hoping.[48] A Seebeck coefficient parallel to the pressing plane of 26 μV K^{-1} can be observed at 1233 K. While the Seebeck coefficient of the FLG nano-flakes perpendicular to the pressing plane showed significantly lower values than parallel to the pressing direction, that also linearly increased, reaching to the maximum value of 11 μV K^{-1} at 1233 K.

Figure 2c shows power factor plots parallel to and perpendicular to the pressing direction. The resulting power factor is seen to increase exponentially as the function of increasing temperature due to both components increasing linearly with temperature. Perpendicular to the pressing direction the values remained substantially low typically below 1 μW m^{-1} K^{-1} until 800 K which exponentially increased between 800 and 1233 K and reached up to 13 μW m^{-1} K^{-1}. While, parallel to the pressing direction exhibited a semi-linear trend and the power factor reached up to 11 μW m^{-1} K^{-1}. The power factor difference between the two planes is due to parallel to the pressing plane having a higher Seebeck coefficient than perpendicular to the pressing plane, but a lower electrical conductivity, which can be explained due to fewer grain boundaries being present perpendicular to the pressing plane.

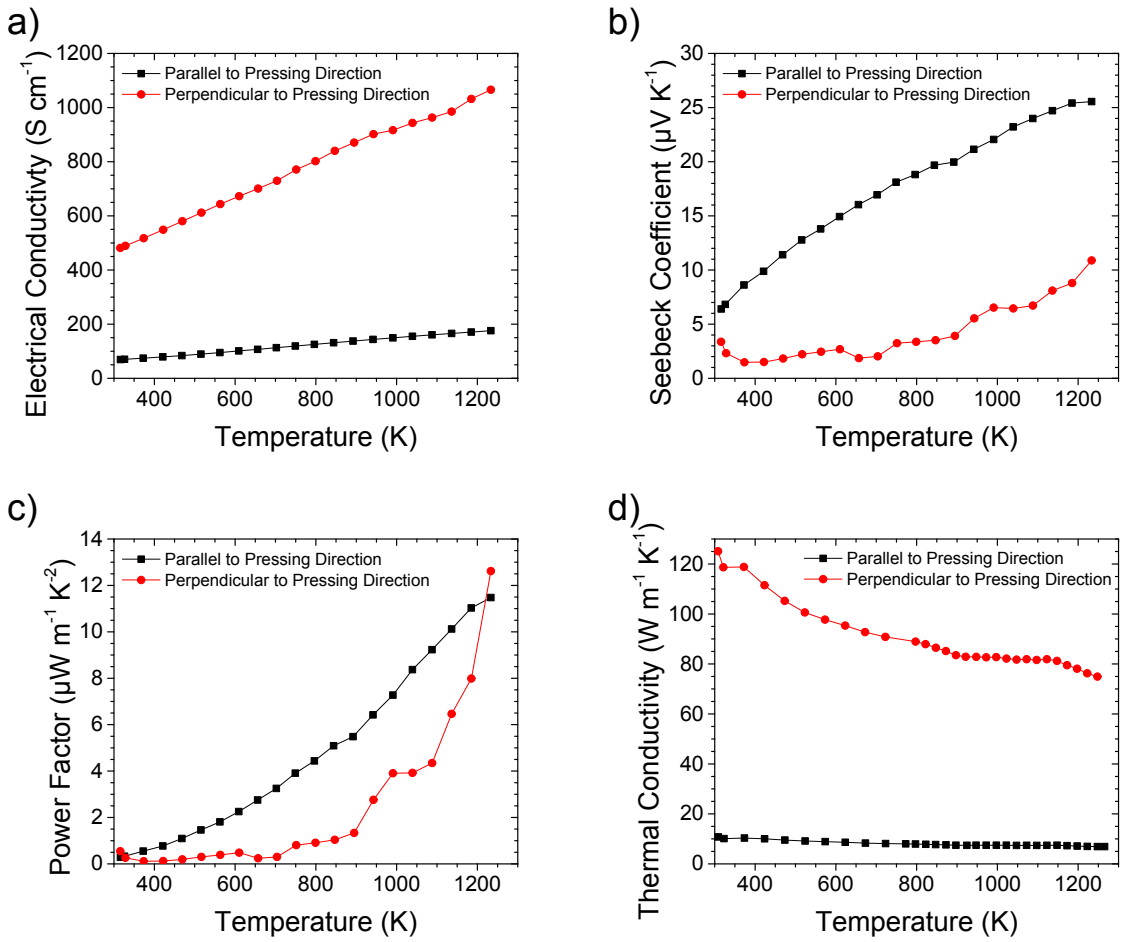

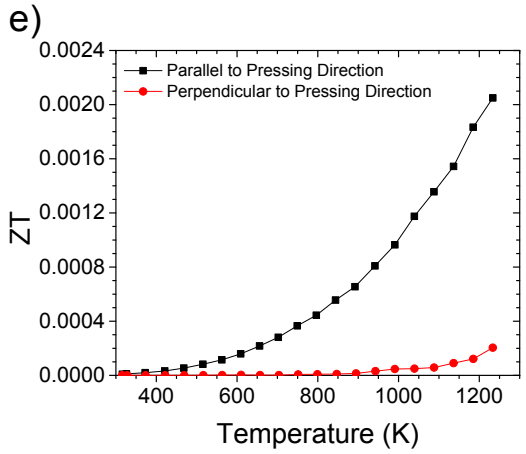

Figure 3: Thermoelectric properties of the FLG nano-flakes based pellets. **(a)** Electrical conductivity, **(b)** Seebeck coefficient, **(c)** power factor **(d)** thermal conductivity and, **(e)** figure of merit, parallel to and perpendicular to the pressing directions.

Thermal conductivity was calculated as the product of heat capacity (**Figure S1a**), thermal diffusivity (**Figure S1b**) and density. **Figure 3d** shows the thermal conductivity parallel to and perpendicular to the pressing direction of the FLG nano-flakes based pellets, which is significantly lower compared to other values reported for FLG [49]. This observation is most likely due to the high numbers of grain boundaries in the bulk pellets compared to isolated FLG samples. The values perpendicular to the pressing direction are substantially higher than parallel to the pressing direction and is 125 W m^{-1} K^{-1} at 308 K that follows a negative linear trend dropping to 75 W m^{-1} K^{-1} at 1233 K. Parallel to the pressing direction shows the same linear decreasing trend as the function of increasing temperature, starting at 11 W m^{-1} K^{-1} at 309 K and decreasing to 7 W m^{-1} K^{-1} at 1266 K. The overall trend is negative with temperature increase, the opposite observation when compared to the electrical conductivity. Thermal conductivity can be expressed as the sum of the electrical and lattice components ($\kappa = \kappa_e + \kappa_L$) and the electrical component is linearly

dependent on the electrical conductivity as shown by Wiedemann-Franz law ($\kappa_e = L.\sigma.T$). The drop in thermal conductivity with increase in temperature can therefore not be explained by the electrical component, but instead must be occurring due to a drop in the lattice component. An explanation for this could be a 'puffing effect' in the bulk FLG pellets due to the thermal expansion of tiny air bubbles between FLGs, leading to increased gaps between FLGs, which increases phonon scattering and thus reduces the lattice component of thermal conductivity. This trend in thermal conductivity and the values observed are similar to polycrystalline graphite,[50] with the perpendicular to plane being higher and the parallel to plane being lower.

The differences in the thermal conductivity, the Seebeck coefficient and the electrical conductivity of FLG between parallel to and perpendicular to the pressing direction could be explained by the FLG plane orientation. The FLG planes line up preferentially perpendicular to the pressing direction, which causes more grain boundaries parallel to the pressing direction than against it. More grain boundaries could equate to lower electrical and thermal conductivity and higher Seebeck coefficient.[51]

Figure 3e determines the dimensionless figure of merit (ZT) parallel to and perpendicular to the pressing directions of the FLG nano-flakes. Although, parallel to the pressing direction, the value is very low at room temperature (9×10^{-6}) the value steadily increases with increasing temperature in an exponential manner to 1188 K where the maximum ZT value of 0.00206 is observed. The simultaneous increase of the electrical conductivity and Seebeck coefficient with increasing temperature and a lowering thermal conductivity at the same time, all indicate higher ZT numbers could be observed at more elevated temperatures, up to graphene's melting point of typically above 4000 K.[52] However, due to instrument limitations measurements could not be conducted above 1273 K. The *ZT* plot perpendicular to the pressing direction shows the trend

similar to the parallel to the pressing direction but it possesses significantly lower values that reached to a maximum of 0.0009 at above 1200 K. Whilst these values are low compared to most inorganic thermoelectric materials and the highest values reported for PEDOT:PSS, they are similar to most organic conducting polymers such as polypyrrole (ZT = 0.0068)[53], P3HT (ZT = 0.04)[54] and Poly[Cux(Cu-ett)] (ZT = 0.014)[55] and polymer composites, such as polythiophene/MWCNT (ZT = 0.000871)[56], PEDOT:PSS/rGO:C_{60} (ZT = 0.067) [57] and P3HT/MWCNT (ZT = 0.00002).[58] The bulk few layer graphene pellets have the potential to achieve higher ZT values through doping and, in contrast to conducting polymers, are stable to over 1273 K and could therefore lead to an organic route harness high grade heat through thermoelectric generators.

3.3 Performance evaluation of FLG nano-flakes based TEGs

Despite the limited ZT in the temperature range studied compared to some inorganic materials, the ease of large-scale production of these organic FLG pellets was used to allow the production of to our knowledge the thickest organic thermoelectric generator legs to date (~0.65 mm). As a proof of concept, the TEGs were fabricated onto a polyester sheet to make use of a flexible substrate to build a flexible TEG, despite the bulky and rigid nature of the pellets. The TEGs composed of only p-type FLG nano-flakes based pellets, glued onto the substate and were connected in series by brush painting silver paint as seen for other materials in the literature.[33] The fabricated device and the corresponding TE performance evaluation have been presented in the **Figure 4a-d** with heat flowing perpendicular to the pressing direction**.** The short circuit current (I_{sc}) and the open circuit voltage (V_{oc}) versus temperature gradient for the single TEG unit has been plotted in **Figure 4c**. While **Figure S2** presents the corresponding plots for the quadruple TEG units. The single TEG unit reached a maximum open circuit voltage (V_{oc}) of 1.30 mV and short

circuit current (I_{sc}) of 0.46 mA corresponding to the maximum power output of 150 nW (assuming $P_{max} = 0.25 \times V_{oc} \times I_{sc}$) [59] while the quadruple TEG units yielded an output power of (V_{oc} = 2.24 mV, I_{sc}= 0.55 mA) 308 nW. However, due to slight heat fluctuations on the samples the voltage and current values were seen to fluctuate by up to 6% each during the measurements, therefore an error bar of ± 12% has been implemented into the data in **Figure 4d**. The voltage generated by each device linearly increased with both the ΔT and the number of pellets connected in series.

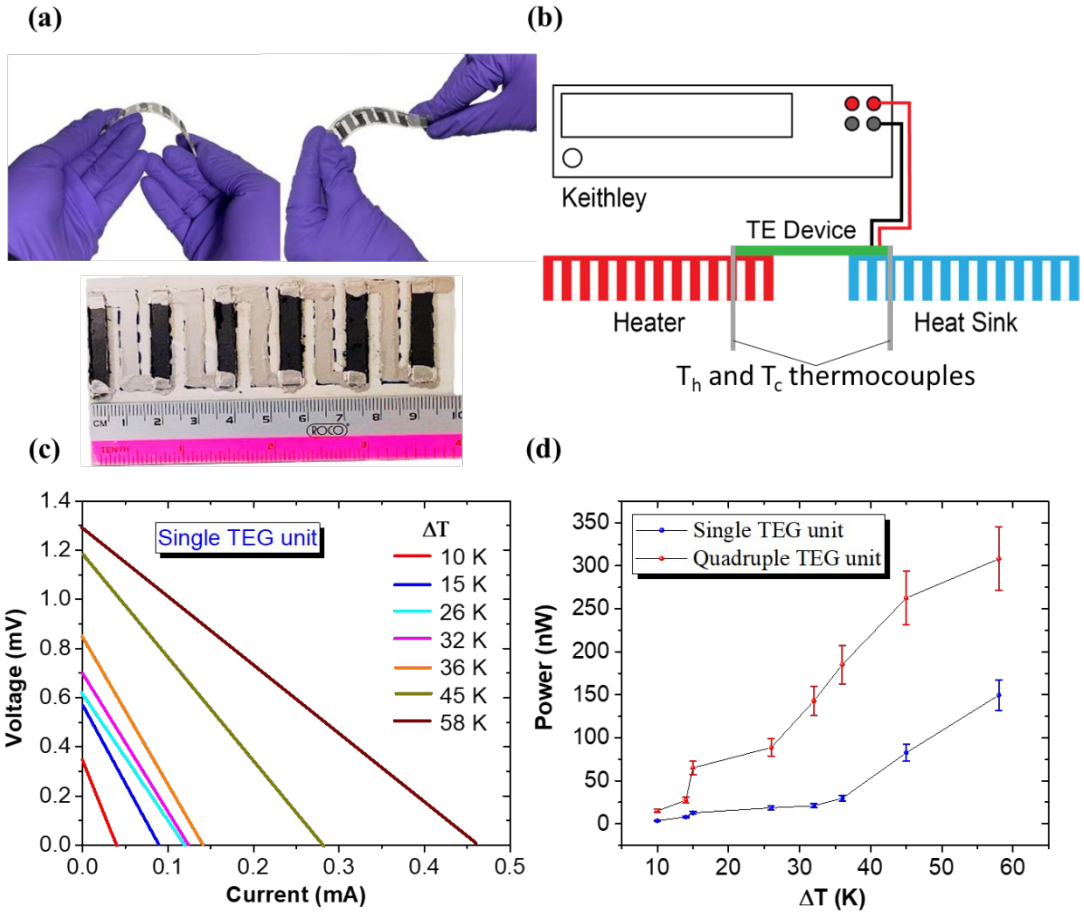

Figure 4: **(a)** Photograph of the fabricated TEGs, **(b)** device testing schematic, **(c)** linearly connected V_{oc} and I_{sc} at different ΔT, **(d)** Maximum power output of the single and quadruple TEG units at various temperature differentials assuming that $P_{max} = 0.25 \times V_{oc} \times I_{sc}$.[59]

Our devices yielded reasonably higher output power up to the temperature gradient of 50 K, which is higher than most organic TEGs reported to date, as shown in **Figure 5**.[60-70] However, for the practical application of FLG nano-flakes based bulk material, device performance is desired to be improved. Such as, by optimizing the device structure (e.g. with heat flow travelling parallel to the pressing direction), reducing contact resistant, or introducing the suitable n-type counterpart. Further improvements could also be yielded by doping the FLG to optimize ZT. Nevertheless, due to the ease of bulk fabrication of FLG, these organic TEGs still exhibit higher power output than any organic TEG in the literature to date with so few legs.

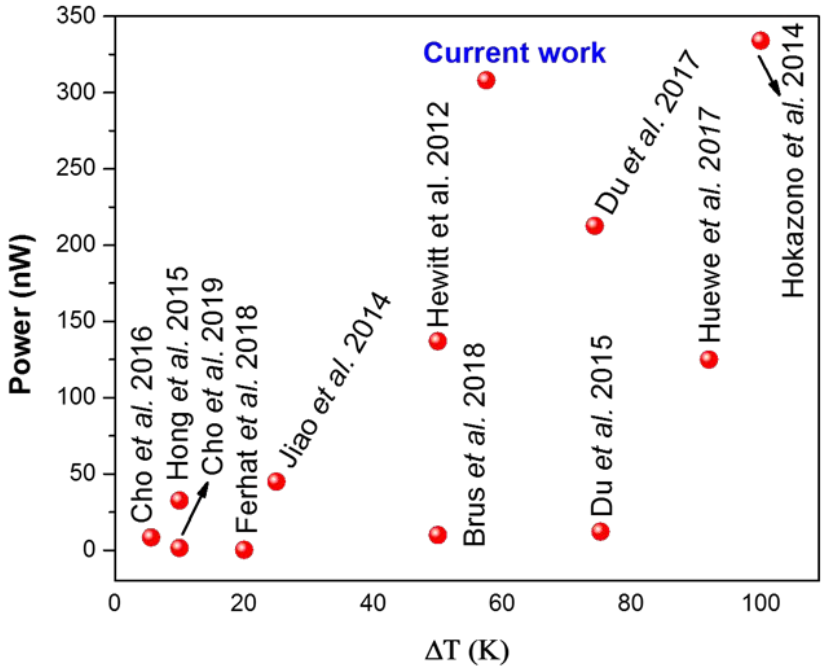

Figure 5: Output power of the recently reported thermoelectric devices based on organic, organic-organic, and organic-inorganic composites materials.

4. CONCLUSIONS

In summary, bulk FLG nano-flakes based pellets were successfully synthesized by a novel physical grinding technique, which exhibited significantly lower thermal conductivity of 7 W m^{-1} K^{-1} at 1266 K compared to FLG values reported in the literature. Low figures of merit compared to inorganic thermoelectric materials of 0.0021 (at 1233 K) parallel to the pressing direction and 0.0002 (at 1233 K) perpendicular to the pressing direction were observed due to the low Seebeck coefficients in the region of 10 μV K^{-1} being measured. A novel proof of concept TEG device was fabricated using the bulk-FLG nano-flakes onto a flexible polyester substrate. Owing to the realization of the bulk FLG nano-flakes fabrication, the TEG devices performed well compared to other organic TEGs, with the output power of a single and quadruple TEG units being 150 and 308 nW, respectively. In addition to the good output power compared to other organic TEGs reported in the literature, it has excellent properties of flexibility (due to the substrate), lightweight and low-cost, which has tremendous potential in the practical wearable applications. Although, the current device yields moderate output power, modules based on the current pellets can be utilized for low and medium power devices. Devices based on FLG could be used in self powered sensors that require little power but require a lightweight and non-toxic TEG. Moreover, the current performance can be improved by optimization of the pellet making process, doping the FLG to optimize the carrier concentration and reducing the contact resistance with better choice of conductive material and the device structure. Moreover, the presented TEG units were fabricated by conceptually simple, environmentally friendly, non-toxic, Earth abundant and scalable process using only organic components in bulk.

ACKNOWLEDGMENTS

We would like to thank the Solar Photovoltaic Academic Research Consortium II (SPARC II) project, funded by WEFO for support. Moreover, the authors acknowledge the SPECIFIC Innovation and Knowledge Centre (EP/N020863/1) for funding. The authors would also like to thank COATED2 (EPSRC EP/L015099/1) for purchasing the ULVAC ZEM-3. The authors wish to thank the Welsh Government, European Regional Development Fund (ERDF) and SMART Expertise Wales for funding Materials Advanced Characterization Centre (MACH1) and Combinatorial Metallurgy (COMET).

SUPPORTING INFORMATION

The Supporting Information is available free of charge on the ACS Publications website at DOI:

- Differential Scanning Calorimetry (DSC) Cp determination.
- Heat capacity values determined from DSC for bulk few layer graphene nano-flakes and diffusivity for bulk few layer graphene nano-flakes both parallel and perpendicular to the pressing direction as determined by LFA.
- Linearly connected V_{oc} and I_{sc} at different ΔT of quadruple TEG units.

REFERENCES

(1) Newell, R. G.; Raimi, D.; Aldana, G. Global Energy Outlook 2019: The Next Generation of Energy. *Resources for the Future* **2019**.

(2) Vaqueiro, P.; Powell, A. V. Recent Developments in Nanostructured Materials for High-Performance Thermoelectrics. *Journal of Materials Chemistry* **2010,** *20* (43), 9577-9584.

(3) Johnson, I.; Choate, W. T.; Davidson, A. *Waste Heat Recovery. Technology and Opportunities in US Industry*; BCS, Inc., Laurel, MD (United States): 2008.

(4) Little, A. B.; Garimella, S. Comparative Assessment of Alternative Cycles for Waste Heat Recovery and Upgrade. *Energy* **2011,** *36* (7), 4492-4504.

(5) He, W.; Zhang, G.; Zhang, X.; Ji, J.; Li, G.; Zhao, X. Recent Development and Application of Thermoelectric Generator and Cooler. *Applied Energy* **2015,** *143*, 1-25.

(6) Xu, S.; Hong, M.; Shi, X.-L.; Wang, Y.; Ge, L.; Bai, Y.; Wang, L.; Dargusch, M.; Zou, J.; Chen, Z.-G. High-Performance PEDOT:PSS Flexible Thermoelectric Materials and Their Devices by Triple Post-Treatments. *Chemistry of Materials* **2019,** *31* (14), 5238-5244.

(7) Liu, W. D.; Chen, Z. G.; Zou, J. Eco-Friendly Higher Manganese Silicide Thermoelectric Materials: Progress and Future Challenges. *Advanced Energy Materials* **2018,** *8* (19), 1800056.

(8) Zebarjadi, M.; Esfarjani, K.; Dresselhaus, M.; Ren, Z.; Chen, G. Perspectives on Thermoelectrics: From Fundamentals to Device Applications. *Energy & Environmental Science* **2012,** *5* (1), 5147-5162.

(9) Snyder, G. J.; Toberer, E. S. Complex Thermoelectric Materials. In Materials for Sustainable Energy: a Collection of Peer-Reviewed Research and Review Articles from Nature Publishing Group; World Scientific: 2011; pp 101-110.

(10) Culebras, M.; Cho, C.; Krecker, M.; Smith, R.; Song, Y.; Gómez, C. M.; Cantarero, A. s.; Grunlan, J. C. High Thermoelectric Power Factor Organic Thin Films through Combination of Nanotube Multilayer Assembly and Electrochemical Polymerization. *ACS applied materials & interfaces* **2017,** *9* (7), 6306-6313.

(11) Cho, C.; Bittner, N.; Choi, W.; Hsu, J. H.; Yu, C.; Grunlan, J. C. Thermally Enhanced n-Type Thermoelectric Behavior in Completely Organic Graphene Oxide-Based Thin Films. *Advanced Electronic Materials* **2018**, 1800465

(12) Burton, M. R.; Mehraban, S.; Beynon, D.; McGettrick, J.; Watson, T.; Lavery, N. P.; Carnie, M. J. 3D Printed SnSe Thermoelectric Generators with High Figure of Merit. *Advanced Energy Materials* **2019**, 1900201

(13) Burton, M. R.; Liu, T.; McGettrick, J.; Mehraban, S.; Baker, J.; Pockett, A.; Watson, T.; Fenwick, O.; Carnie, M. J. Thin Film Tin Selenide (SnSe) Thermoelectric Generators Exhibiting Ultralow Thermal Conductivity. *Advanced Materials* **2018,** *30* (31), 1801357.

(14) Leclerc, M.; Najari, A. Organic Thermoelectrics: Green Energy from a Blue Polymer. *Nature materials* **2011,** *10* (6), 409.

(15) Kroon, R.; Mengistie, D. A.; Kiefer, D.; Hynynen, J.; Ryan, J. D.; Yu, L.; Müller, C. Thermoelectric Plastics: From Design to Synthesis, Processing and Structure–Property Relationships. *Chemical Society Reviews* **2016,** *45* (22), 6147-6164.

(16) Fan, Z.; Li, P.; Du, D.; Ouyang, J. Significantly Enhanced Thermoelectric Properties of PEDOT: PSS Films through Sequential Post-Treatments with Common Acids and Bases. *Advanced Energy Materials* **2017,** *7* (8), 1602116.

(17) Dey, A.; Hadavale, S.; Khan, M. A. S.; More, P.; Khanna, P. K.; Sikder, A. K.; Chattopadhyay, S. Polymer Based Graphene/Titanium Dioxide Nanocomposite (GTNC): An Emerging and Efficient Thermoelectric Material. *Dalton Transactions* **2015,** *44* (44), 19248-19255.

(18) Dey, A.; Bajpai, O. P.; Sikder, A. K.; Chattopadhyay, S.; Khan, M. A. S. Recent Advances in CNT/Graphene Based Thermoelectric Polymer Nanocomposite: A Proficient Move Towards Waste Energy Harvesting. *Renewable and sustainable energy reviews* **2016,** *53*, 653-671.

(19) Dey, A.; Maity, A.; Khan, M. A. S.; Sikder, A. K.; Chattopadhyay, S. PVAc/PEDOT: PSS/Graphene–Iron Oxide Nanocomposite (GINC): An Efficient Thermoelectric Material. *RSC advances* **2016,** *6* (27), 22453-22460.

(20) Hsieh, Y.-Y.; Zhang, Y.; Zhang, L.; Fang, Y.; Kanakaraaj, S. N.; Bahk, J.-H.; Shanov, V. High Thermoelectric Power-Factor Composites Based on Flexible Three-Dimensional Graphene and Polyaniline. *Nanoscale* **2019,** *11* (14), 6552-6560.

(21) Kim, G. H.; Shao, L.; Zhang, K.; Pipe, K. P. Engineered Doping of Organic Semiconductors for Enhanced Thermoelectric Efficiency. *Nature materials* **2013,** *12* (8), 719.

(22) Geim, A. K.; Novoselov, K. S., Nature Mater. 6, 183 (2007). 2010.

(23) Bonaccorso, F.; Sun, Z.; Hasan, T.; Ferrari, A. Graphene Photonics and Optoelectronics. *Nature photonics* **2010,** *4* (9), 611.

(24) Wang, Y.; Yang, J.; Wang, L.; Du, K.; Yin, Q.; Yin, Q. Polypyrrole/Graphene/Polyaniline Ternary Nanocomposite with High Thermoelectric Power Factor. *ACS applied materials & interfaces* **2017,** *9* (23), 20124-20131.

(25) Dollfus, P.; Nguyen, V. H.; Saint-Martin, J. Thermoelectric Effects in Graphene Nanostructures. *Journal of Physics: Condensed Matter* **2015,** *27* (13), 133204.

(26) Pop, E.; Varshney, V.; Roy, A. K. Thermal Properties of Graphene: Fundamentals and Applications. *MRS bulletin* **2012,** *37* (12), 1273-1281.

(27) Ouyang, Y.; Guo, J. A Theoretical study on Thermoelectric Properties of Graphene Nanoribbons. *Applied Physics Letters* **2009,** *94* (26), 263107.

(28) Yokomizo, Y.; Nakamura, J. Giant Seebeck Coefficient of the Graphene/h-BN Superlattices. *Applied Physics Letters* **2013,** *103* (11), 113901.

(29) Chang, P.-H.; Nikolić, B. K. Edge Currents and Nanopore Arrays in Zigzag and Chiral Graphene Nanoribbons as a Route Toward High-ZT Thermoelectrics. *Physical Review B* **2012,** *86* (4), 041406.

(30) Juntunen, T.; Jussila, H.; Ruoho, M.; Liu, S.; Hu, G.; Albrow-Owen, T.; Ng, L. W.; Howe, R. C.; Hasan, T.; Sun, Z. Inkjet Printed Large-Area Flexible Few-Layer Graphene Thermoelectrics. *Advanced Functional Materials* **2018,** *28* (22), 1800480.

(31) Chen, G.; Xu, W.; Zhu, D. Recent Advances in Organic Polymer Thermoelectric Composites. *Journal of Materials Chemistry C* **2017,** *5* (18), 4350-4360.

(32) Guo, Y.; Mu, J.; Hou, C.; Wang, H.; Zhang, Q.; Li, Y. Flexible and Thermostable Thermoelectric Devices Based on Large-Area and Porous All-Graphene Films. *Carbon* **2016,** *107*, 146-153.

(33) Eom, Y.; Wijethunge, D.; Park, H.; Park, S. H.; Kim, W. Flexible Thermoelectric Power Generation System Based on Rigid Inorganic Bulk Materials. *Applied energy* **2017,** *206*, 649-656.

(34) Lindemann, A.; Beckstein, F.; Brunner, M. Penetration Model in the NETZSCH LFA Software− Porous Materials Finally Handled Properly!

(35) Smakula, A.; Sils, V. Precision Density Determination of Large Single Crystals by Hydrostatic Weighing. *Physical Review* **1955,** *99* (6), 1744.

(36) Rao, K. S.; Senthilnathan, J.; Liu, Y.-F.; Yoshimura, M. Role of Peroxide Ions in Formation of Graphene Nanosheets by Electrochemical Exfoliation of Graphite. *Scientific reports* **2014,** *4*, 4237.

(37) Ferrari, A. C.; Meyer, J.; Scardaci, V.; Casiraghi, C.; Lazzeri, M.; Mauri, F.; Piscanec, S.; Jiang, D.; Novoselov, K.; Roth, S. Raman Spectrum of Graphene and Graphene Layers. *Physical review letters* **2006,** *97* (18), 187401.

(38) Peng, K.-J.; Wu, C.-L.; Lin, Y.-H.; Liu, Y.-J.; Tsai, D.-P.; Pai, Y.-H.; Lin, G.-R. Hydrogen-free PECVD Growth of Few-Layer Gaphene on an Ultra-Thin Nickel Film at the Threshold Dissolution Temperature. *Journal of Materials Chemistry C* **2013,** *1* (24), 3862-3870.

(39) Gautam, M.; Shi, Z.; Jayatissa, A. H. Graphene Films as Transparent Electrodes for Photovoltaic Devices Based on Cadmium Sulfide Thin Films. *Solar Energy Materials and Solar Cells* **2017,** *163*, 1-8.

(40) Lin, P.-C.; Wu, J.-Y.; Liu, W.-R. Green and Facile Synthesis of Few-Layer Graphene via Liquid Exfoliation Process for Lithium-ion Batteries. *Scientific reports* **2018,** *8* (1), 9766.

(41) Paton, K. R.; Varrla, E.; Backes, C.; Smith, R. J.; Khan, U.; O'Neill, A.; Boland, C.; Lotya, M.; Istrate, O. M.; King, P. Scalable Production of Large Quantities of Defect-Free Few-Layer Graphene by Shear Exfoliation in Liquids. *Nature materials* **2014,** *13* (6), 624.

(42) Noroozi, M.; Zakaria, A.; Radiman, S.; Wahab, Z. A. Environmental Synthesis of Few Layers Graphene Sheets Using Ultrasonic Exfoliation with Enhanced Electrical and Thermal Properties. *PloS one* **2016,** *11* (4).

(43) González-Domínguez, J. M.; León, V.; Lucío, M. I.; Prato, M.; Vázquez, E. Production of Ready-to-use Few-Layer Graphene in Aqueous Suspensions. *Nature protocols* **2018,** *13* (3), 495.

(44) Sawant, S. Y.; Somani, R. S.; Cho, M. H.; Bajaj, H. C. A Low Temperature Bottom-up Approach for the Synthesis of Few Layered Graphene Nanosheets via C–C Bond Formation Using a Modified Ullmann Reaction. *RSC Advances* **2015,** *5* (58), 46589-46597.

(45) Wu, Y.; Wang, B.; Ma, Y.; Huang, Y.; Li, N.; Zhang, F.; Chen, Y. Efficient and Large-Scale Synthesis of Few-Layered Graphene Using an Arc-discharge Method and Conductivity Studies of the Resulting Films. *Nano Research* **2010,** *3* (9), 661-669.

(46) Snyder, G.; Toberer, E. Complex Thermoelectric Materials. nature materials, v. 7. **2008**.

(47) Park, H. J.; Meyer, J.; Roth, S.; Skákalová, V. Growth and Properties of Few-Layer Graphene Prepared by Chemical Vapor Deposition. *Carbon* **2010,** *48* (4), 1088-1094.

(48) Babichev, A.; Gasumyants, V.; Butko, V., Resistivity and Thermopower of Graphene Made by Chemical Vapor Deposition Technique. American Institute of Physics: 2013.

(49) Ghosh, S.; Bao, W.; Nika, D. L.; Subrina, S.; Pokatilov, E. P.; Lau, C. N.; Balandin, A. A. Dimensional Crossover of Thermal Transport in Few-Layer Graphene. *Nature materials* **2010,** *9* (7), 555-558.

(50) Zhang, G.; Zhao, J.; Chow, P. C.; Jiang, K.; Zhang, J.; Zhu, Z.; Zhang, J.; Huang, F.; Yan, H. Nonfullerene Acceptor Molecules for Bulk Heterojunction Organic Solar Cells. *Chemical reviews* **2018,** *118* (7), 3447-3507.

(51) Takashiri, M.; Miyazaki, K.; Tanaka, S.; Kurosaki, J.; Nagai, D.; Tsukamoto, H. Effect of Grain Size on Thermoelectric Properties of n-type Nanocrystalline Bismuth-Telluride Based Thin Films. *Journal of Applied Physics* **2008,** *104* (8), 084302.

(52) Ganz, E.; Ganz, A. B.; Yang, L.-M.; Dornfeld, M. The Initial Stages of Melting of Graphene Between 4000 K and 6000 K. *Physical Chemistry Chemical Physics* **2017,** *19* (5), 3756-3762.

(53) Culebras, M.; Uriol, B.; Gómez, C. M.; Cantarero, A. Controlling the Thermoelectric Properties of Polymers: Application to PEDOT and Polypyrrole. *Physical Chemistry Chemical Physics* **2015,** *17* (23), 15140-15145.

(54) Zhang, Q.; Sun, Y.; Xu, W.; Zhu, D. Thermoelectric Energy from Flexible P3HT Films Doped with a Ferric Salt of Triflimide Anions. *Energy & Environmental Science* **2012,** *5* (11), 9639-9644.

(55) Sun, Y.; Sheng, P.; Di, C.; Jiao, F.; Xu, W.; Qiu, D.; Zhu, D. Organic Thermoelectric Materials and Devices Based on P-and N-Type Poly (metal 1, 1, 2, 2-ethenetetrathiolate) s. *Advanced Materials* **2012,** *24* (7), 932-937.

(56) Wang, L.; Jia, X.; Wang, D.; Zhu, G.; Li, J. Preparation and Thermoelectric Properties of Polythiophene/Multiwalled Carbon Nanotube Composites. *Synthetic metals* **2013,** *181*, 79-85.

(57) Zhang, K.; Zhang, Y.; Wang, S. Enhancing Thermoelectric Properties of Organic Composites through Hierarchical Nanostructures. *Scientific reports* **2013,** *3*, 3448.

(58) Bounioux, C.; Díaz-Chao, P.; Campoy-Quiles, M.; Martín-González, M. S.; Goni, A. R.; Yerushalmi-Rozen, R.; Müller, C. Thermoelectric Composites of Poly (3-hexylthiophene) and Carbon Nanotubes with a Large Power Factor. *Energy & Environmental Science* **2013,** *6* (3), 918-925.

(59) Fan, P.; Zheng, Z.-h.; Li, Y.-z.; Lin, Q.-y.; Luo, J.-t.; Liang, G.-x.; Cai, X.-m.; Zhang, D.-p.; Ye, F. Low-Cost Flexible Thin Film Thermoelectric Generator on Zinc Based Thermoelectric Materials. *Applied Physics Letters* **2015,** *106* (7), 073901.

(60) Huewe, F.; Steeger, A.; Kostova, K.; Burroughs, L.; Bauer, I.; Strohriegl, P.; Dimitrov, V.; Woodward, S.; Pflaum, J. Low-Cost and Sustainable Organic Thermoelectrics Based on Low-Dimensional Molecular Metals. *Advanced Materials* **2017,** *29* (13), 1605682.

(61) Ferhat, S.; Domain, C.; Vidal, J.; Noël, D.; Ratier, B.; Lucas, B. Organic Thermoelectric Devices Based on a Stable N-type Nanocomposite Printed on Paper. *Sustainable Energy & Fuels* **2018,** *2* (1), 199-208.

(62) Hong, C. T.; Kang, Y. H.; Ryu, J.; Cho, S. Y.; Jang, K.-S. Spray-Printed CNT/P3HT Organic Thermoelectric Films and Power Generators. *Journal of Materials Chemistry A* **2015,** *3* (43), 21428-21433.

(63) Cho, C.; Wallace, K. L.; Tzeng, P.; Hsu, J. H.; Yu, C.; Grunlan, J. C. Outstanding low Temperature Thermoelectric Power Factor from Completely Organic Thin Films Enabled by Multidimensional Conjugated Nanomaterials. *Advanced Energy Materials* **2016,** *6* (7), 1502168.

(64) Brus, V. V.; Gluba, M.; Rappich, J. r.; Lang, F.; Maryanchuk, P. D.; Nickel, N. H. Fine Art of Thermoelectricity. *ACS applied materials & interfaces* **2018,** *10* (5), 4737-4742.

(65) Hewitt, C. A.; Kaiser, A. B.; Roth, S.; Craps, M.; Czerw, R.; Carroll, D. L. Multilayered Carbon Nanotube/Polymer Composite Based Thermoelectric Fabrics. *Nano letters* **2012,** *12* (3), 1307-1310.

(66) Cho, C.; Bittner, N.; Choi, W.; Hsu, J. H.; Yu, C.; Grunlan, J. C. Thermally Enhanced n-Type Thermoelectric Behavior in Completely Organic Graphene Oxide-Based Thin Films. *Advanced Electronic Materials* **2019,** *5* (11), 1800465.

(67) Hokazono, M.; Anno, H.; Toshima, N. Thermoelectric Properties and Thermal Stability of PEDOT:PSS Films on a Polyimide Substrate and Application in Flexible Energy Conversion Devices. *Journal of electronic materials* **2014,** *43* (6), 2196-2201.

(68) Jiao, F.; Di, C.-a.; Sun, Y.; Sheng, P.; Xu, W.; Zhu, D. Inkjet-Printed Flexible Organic Thin-Film Thermoelectric Devices Based on P-and N-type Poly (metal 1, 1, 2, 2-ethenetetrathiolate) s/Polymer Composites through Ball-Milling. *Philosophical Transactions of the Royal Society A: Mathematical, Physical and Engineering Sciences* **2014,** *372* (2013), 20130008.

(69) Du, Y.; Cai, K.; Chen, S.; Wang, H.; Shen, S. Z.; Donelson, R.; Lin, T. Thermoelectric Fabrics: Toward Power Generating Clothing. *Scientific reports* **2015,** *5*, 6411.

(70) Du, Y.; Cai, K.; Shen, S.; Donelsonand, R.; Xu, J.; Wang, H.; Lin, T. Multifold Enhancement of the Output Power of Flexible Thermoelectric Generators Made from Cotton Fabrics Coated with Conducting polymer. *RSC advances* **2017,** *7* (69), 43737-43742.

Table of Contents graphic